35-GHz Barium Hexaferrite/PDMS Composite-Based Millimeter-Wave Circulators for 5G Applications

Renuka Bowrothu, *Member, IEEE*, Hae-In Kim, *Member, IEEE*, Connor S. Smith, *Graduate Student Member, IEEE*, David P. Arnold, *Senior Member, IEEE*, and Yong-Kyu Yoon, *Member, IEEE*

***Abstract*— We report a self-biased, low-profile circulator operating in the Ka-band fabricated by an entirely low-temperature (70 °C) screen-printing approach on printed circuit board (PCB). The magnetic material for the circulator is a barium hexaferrite BaFe12O19 (BaM)/polydimethylsiloxane (PDMS) nanocomposite that exhibits a zero-bias ferromagnetic resonance frequency (f_{FMR}) at 46.6 GHz. Using this material, a microstrip-based circulator operating at 35 GHz is designed, fabricated, and characterized. A combination of mechanical milling, screen printing, photolithography, and electroplating is used for fabricating the circulator, in which the circulator disk (diameter of 2 mm and thickness of 250 μm) is completely embedded in the PCB, realizing a packaging compatible low-profile architecture with the total device area of 33 mm^2. The measured isolation (IS) and insertion loss (IL) of the fabricated circulator at 35 GHz is 3.9 and 8.7 dB, respectively. When the additional magnetic bias is applied to the circulator using external permanent magnets, the IS and IL performance is improved to be 7.4 and 8.4 dB, respectively. The impact of the loss factors associated with dielectric loss and surface roughness on the device performance is analyzed using High Frequency Structural Simulator (HFSS).**

***Index Terms*— Barium hexaferrite (BaM) and polydimethylsiloxane (PDMS) composite, dielectric loss, fifth generation (5G), Ka-band, low profile, packaging compatible, roughness effect, screen printing, self-biased circulator.**

I. Introduction

THE Internet of Things (IoT) is one of the rapidly evolving technologies in the modern world. It is estimated that by 2020, nearly 50 billion IoT devices will be connected [1]. To reduce interference and increase bandwidth, data rate, and network speed, current IoT standards are switching from the fourth-generation (4G) to fifth-generation (5G) technology. In 4G technology, Internet protocols (IPs) are operated using packet switching and a data rate of almost 100 Mb/s for mobile networks and 1 Gb/s for local wireless networks [2]. Meanwhile, 5G technology is aiming for higher data rates (>1 Gb/s), machine-to-machine communications between heterogeneous devices with minimum human intervention [3], high bandwidth, and low latency. To meet 5G standards, the U.S. Federal Communications Commission (FCC) has newly launched three 5G bands in the frequency spectrum: below 6 and 24–38 GHz and above 60 GHz. From the device performance perspective compact, high power handling, low loss, and complementary metal–oxide–semiconductor (CMOS) technology compatible RF components, such as antennas, filters, and circulators, are highly recommended.

Circulators are one of the crucial three-port components in an RF front-end module to enable simultaneous transmit and receive (STAR) function via nonreciprocal operation. Currently, nonreciprocity can be achieved by using transistor-/circuit-based approaches [4] that are compatible with CMOS technology and are exercised at low gigahertz frequencies. Although the implementation of active circulators at millimeter-wave (mm-wave) frequencies (>20 GHz) is rapidly revolving [5], [6], in this work, we mainly focus on integrated nonreciprocal passive devices. Alternatively, metamaterial-based nonreciprocal devices have been reported [7], but these devices suffer from poor noise performance, limited power handling capability, and strong nonlinearity [8]. Traditionally, circulators designed using magnetic materials at lower frequencies (<20 GHz) have been successfully demonstrated [9], [10] where external dc bias magnetic field is applied using a permanent magnet to align the magnetic domains of the circulator ferrite. However, as the operational frequency increases especially in K and Ka bands, the strength of the required external field bias also increases, causing the system to be bulky with heavy permanent magnets and not readily compatible with monolithic microwave integrated circuit (MMIC) technologies. On the other hand, barium and strontium hexaferrites (BaM and SrM) possess high crystalline anisotropy, high saturation, and remanent magnetization that allow the magnetic domains to be polarized without the external bias field, and circulators with such magnetic materials are often termed self-biased circulators. These magnetic materials

Manuscript received May 13, 2020; revised July 16, 2020; accepted August 1, 2020. Date of publication September 22, 2020; date of current version December 3, 2020. This work was supported in part by the Defense Advanced Research Project Agency (DARPA/MTO Program) under ARO Grant W911NF-17-1-0050. *(Corresponding author: Renuka Bowrothu.)*

The authors are with the Interdisciplinary Microsystems Group (IMG), Department of Electrical and Computer Engineering, University of Florida, Gainesville, FL 32611 USA (e-mail: rbowrothu93@ufl.edu; connor.smith@ufl.edu; darnold@ufl.edu; ykyoon@ece.ufl.edu).

Color versions of one or more of the figures in this article are available online at https://ieeexplore.ieee.org.

Digital Object Identifier 10.1109/TMTT.2020.3022556

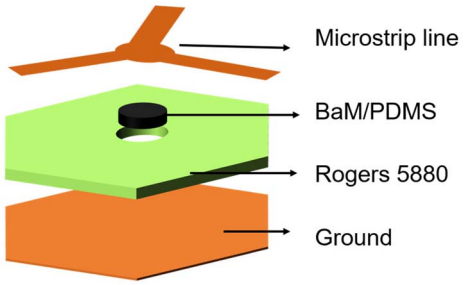

Fig. 1. Schematic of a BaM/PDMS composite-based low-profile, packaging compatible, millimeter-wave circulator.

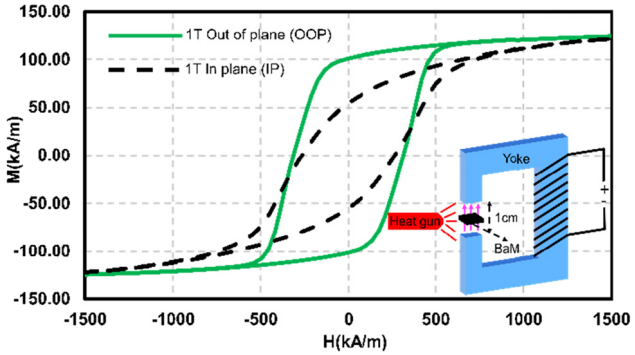

Fig. 2. Demagnetization corrected dc hysteresis of the BaM/PDMS composite.

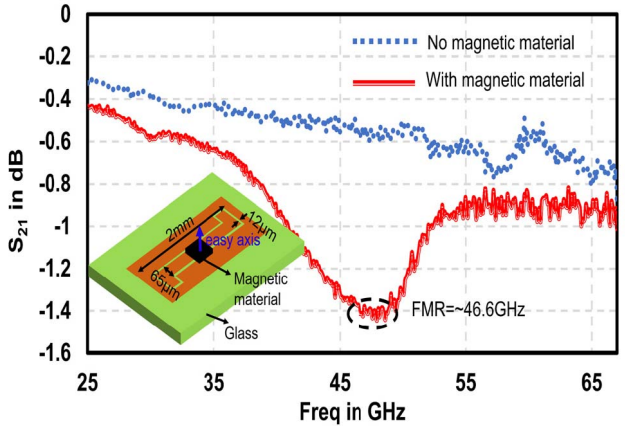

Fig. 3. S_{21} measurements with and without magnetic material.

offer a high ferromagnetic resonance (FMR) frequency and are highly advantageous for mm-wave (including K, Ka, and V bands) devices and applications.

The deposition of these self-biased films has been demonstrated using different techniques, such as a conventional high-temperature ceramic fabrication method [11], a sol–gel process [12], and a vacuum-based dc sputtering process [13] where magnetic films can be deposited in different thicknesses ranging from 1 to 10 μm. Chen *et al.* [14] reported the characterization of screen-printed barium hexaferrite films of thickness ranging between 100 and 400 μm but have not demonstrated any circulator performance. Also, all the reported processes [11]–[14] have utilized sintering or high-temperature annealing, i.e., about 800 °C–1300 °C, prohibiting process compatibility with CMOS semiconductor fabrication technology or organic printing circuit board technology.

In this article, we demonstrate an mm-wave low-temperature processed (∼70 °C) and microfabricated self-biased circulator using barium hexaferrite BaFe12O19 (BaM)/polydimethylsiloxane (PDMS) composites embedded in a Rogers 5880 printed circuit board (PCB) substrate (see Fig. 1), whose thickness is 250 μm. First, the magnetic properties of the BaM/PDMS composite material are characterized using coplanar waveguide (CPW) transmission lines for RF characterization and vibrating sample magnetometer (VSM) techniques for dc magnetic hysteresis analysis. Then, a circulator operating at Ka bands using the BaM/PDMS composite is designed and microfabricated using a 250-μm-thick Rogers 5880 ($\varepsilon_r = 2.2$ and $\tan\delta = 0.0009$ at 10 GHz) PCB substrate. RF performance of the circulator is characterized with and without an additional permanent Nd–Fe–B bias magnet applied on the device.

II. Characterization of Barium Hexaferrite and PDMS Composite

Screen-printed magnetic structures are prepared by mixing 70 wt% BaM, i.e., 30% volume (Nanostructured & Amorphous Materials, Inc.) hexagonal platelets of average diameter 500 nm with 30 wt%, i.e., 70% volume PDMS (Dow Corning Sylgard 184 Silicon) binder consisting of 10:1 ratio of monomer to curing agent. An approximately 1-T magnetic bias field is applied using an iron yoke electromagnet, while the BaM/PDMS composite is cured at 70 °C for 12 h. After the curing step using VSM (ADE Technologies EV9 with a maximum applied field of ±1800 kA/m), the demagnetized dc hysteresis of the composite is measured and plotted, as shown in Fig. 2. The net internal field (H_{int}) is calculated by $H_{\text{int}} = H_{\text{applied}} - N_d M$, where N_d is the demagnetization factor that is taken as 0 for in plane and 1 for out of plane (OOP) and M is the measured magnetization field. The FMR of the material is experimentally determined by using CPW transmission line test structures that are fabricated on a low-loss glass substrate. BaM/PDMS composite material that is 150 μm thick is screen printed on the transmission line, and two-port responses with and without the BaM/PDMS composite are characterized, as shown in Fig. 3. Due to the strong FMR of the BaM/PDMS sample, a peak insertion loss (IL) at 46.6 GHz is observed.

The effective permittivity of BaM/PDMS composite (ε_{eff}) is calculated as [15]

$$\frac{\varepsilon_{\text{eff}} - \varepsilon_{\text{PDMS}}}{\varepsilon_{\text{eff}} + 2\varepsilon_{\text{PDMS}}} = f\frac{\varepsilon_{\text{BaM}} - \varepsilon_{\text{PDMS}}}{\varepsilon_{\text{BaM}} + 2\varepsilon_{\text{PDMS}}} \tag{1}$$

where $\varepsilon_{\text{BaM}} = 14$ and $\varepsilon_{\text{PDMS}} = 2.69$ are the assumed effective permittivity of BaM [16] and PDMS [17], respectively; f is the fractional volume occupied by BaM nanoparticles in PDMS and the dielectric loss tangent of PDMS composite is taken as 0.045 from [18]. Therefore, using (1), the effective permittivity of the BaM/PDMS composite is calculated

TABLE I
EXTRACTED PROPERTIES OF THE SCREEN PRINTED BAM/PDMS COMPOSITE

Parameter	Value
Saturation Magnetization	121 kA/m
Coercivity OOP	324 kA/m
Remanence	101 kA/m
Squareness (M_r/M_s) OOP	0.83
Anisotropy Field	1499 kA/m
Line Width	344.5 KA/m (4330 Oe)
Effective Relative Dielectric Constant	~5
Effective Relative Permeability	1.1

to be 5. Table I summarizes the extracted magnetic and electrical parameters of BaM/PDMS nanocomposite from our test structures. Based on the measured magnetic properties and the FMR frequency, a circulator is designed and fabricated at 35 GHz, i.e., one of the frequency bands for 5G applications.

III. CIRCULATOR DESIGN AND FABRICATION

The extracted magnetic parameters are used to design a circulator below f_{FMR} using analytical equations and High Frequency Structural Simulator (HFSS; ANSYS Inc.). The radius (R) of the ferrite sets the operational frequency of the circulator and is given by the following equation [19]:

$$R = \frac{1.84}{\omega\sqrt{\varepsilon_0\varepsilon_r\mu_0\mu_{\mathrm{eff,composite}}}} \tag{2}$$

where ω is the angular frequency, ε_0 is the permittivity of free space, ε_r is the relative/effective dielectric constant of the ferrite, μ_0 is the vacuum permeability, and $\mu_{\mathrm{eff,composite}}$ is the effective permeability of the BaM/PDMS composite, which is approximated to 1.1. The simulated radius of the composite at 35 GHz is 1.02 mm. The relationship between the central conductor disk and the microstrip linewidth (w) is given by the port suspension angle (2ψ), i.e., $w = 2R\sin\psi$, where 2ψ is calculated using [16]

$$\frac{\sin^2\psi}{\psi} = \frac{\pi * z_d}{\sqrt{3} * 1.848 * Z_{\mathrm{eff}}}\left|\frac{\kappa}{\mu}\right| \tag{3}$$

where κ and μ are the Polder tensor elements of the ferrite [16], Z_{eff} is the intrinsic wave impedance of the ferrite, and z_d is the impedance of the surrounding dielectric material, both of which are calculated from [16]. For the on-chip probe measurement purpose, the microstrip-to-grounded CPW (GCPW) transition is implemented, as shown in Fig. 4.

Based on simulation results, the circulator dimension is fine-tuned and microfabricated, as shown in Fig. 5. First, 400-μm-wide vias for ground connection and a 2.04-mm-wide single via for a circulator are drilled using milling machine followed by Cu clad etching using ferric chloride. After screen printing, the sample is heated at 70 °C for 12 h to cure the BaM/PDMS composite, while a magnetic dc bias field of approximately 1 T is applied to the sample OOP by

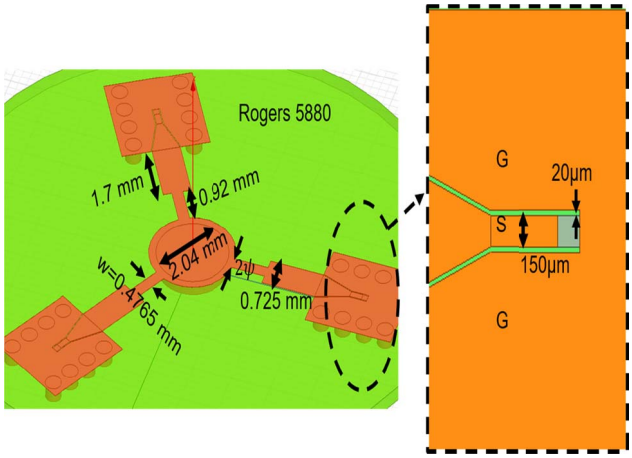

Fig. 4. Schematic of a BaM/PDMS composite-based circulator with designed dimensions: GCPW-to-microstrip transition is used for on-chip probing.

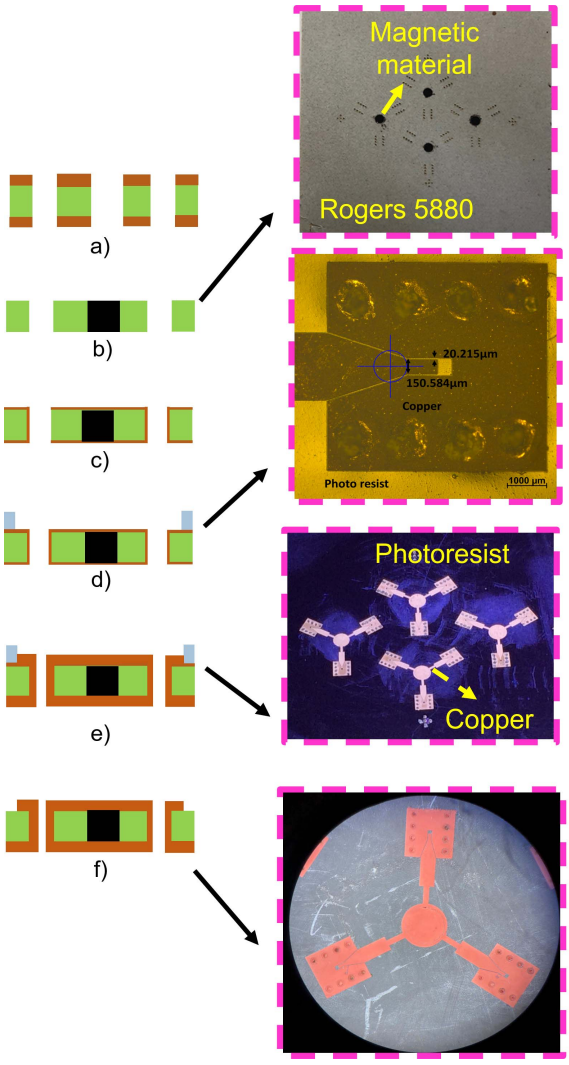

Fig. 5. Fabrication process and fabricated devices. a) Via drilling on 250um Rogers 5880 board. b) Copper etching and magnetic material screen printing. c) 30 nm Ti/500 nm Cu sputtering. d) Patterning using dry film lithography. e) Copper electroplating. f) PR and seed layer removal.

the electromagnet. Next, using dc sputtering, a 500-nm-thick copper (Cu) seed layer is deposited for electroplating and 30-nm-thick titanium (Ti) is used as an adhesion promotion

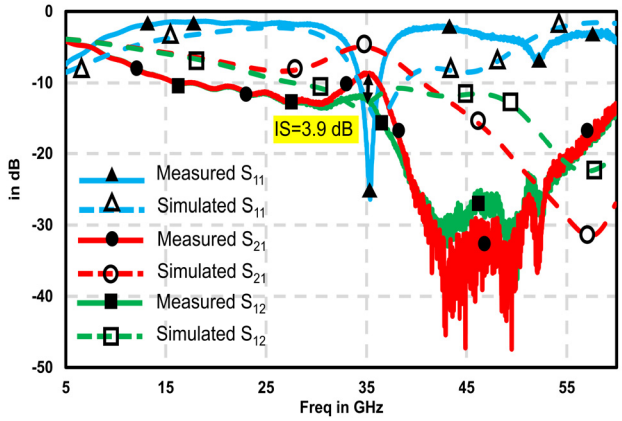

Fig. 6. Measured and simulated S-parameter results.

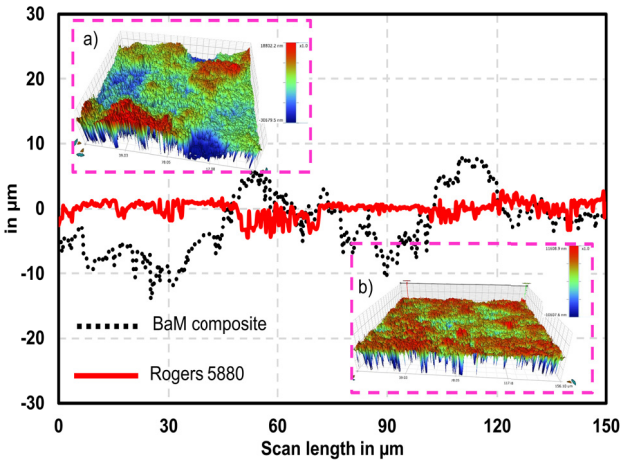

Fig. 7. Surface roughness measurements of the BaM/PDMS composite and Rogers 5880. Inset—(a) BaM/PDMS and (b) Rogers 5880 surface topology.

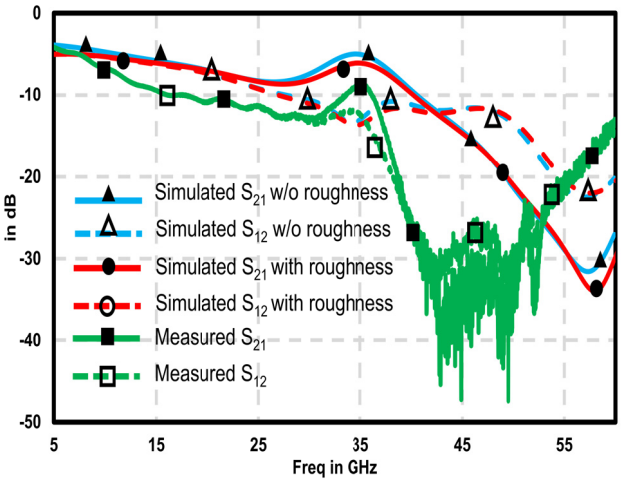

Fig. 8. Surface roughness effect on device performance.

layer. Dupont MX5000 series dry film photoresist (PR) is laminated for photolithography patterning and development. Vacuum-based metal deposition techniques, such as sputtering or evaporation, have a low deposition rate in the order of 0.1–1 nm/s. For high deposition rate and effective via sidewall coverage, electroplating technique is used. A commercial Technic Cu bath with additives and brighteners is used for smooth plating. At a current density of 10 mA/cm^2 for 2 h, the total metal thickness deposited on both sides of the sample is approximately 10 μm. The temperature of the plating bath is set to 38 °C and the stirring rate is 60 r/min. Finally, Dynaloy flipstrip 7000 LOR resist is used to remove the dry film followed by etching the seed layer of Cu and Ti sequentially. A complete fabricated device is shown in Fig. 5. Since PDMS undergoes depolymerization between 450 °C and 650 °C [20], based on PDMS properties [21], this circulator can withstand temperature up to 350 °C.

IV. RF Measurement and Analysis

RF characterization of the fabricated circulators is performed between 5 and 60 GHz using a vector network analyzer (VNA) (HP E8316A, Agilent Inc.). A standard short/open/load/through (SOLT) calibration is performed before two-port measurements are taken. Port 2 of the circulator is terminated with a 50-Ω terminator and RF measured response is shown in Fig. 6. It can be observed that the measured operating frequency (35.2 GHz) of the circulator matches well with the targeted one. Also, the nonreciprocity is clearly observed since the S_{12} and S_{21} values at the operation frequency are different. The simulated isolation (IS) at all the three ports (IS $= S_{21}$–S_{12}) is 8.31 dB, whereas in case of the measured results, isolation varies between 3.04 and 1 dB among all the three ports. This variation in isolation is likely due to the nonuniform distribution of magnetic particles in the BaM/PDMS composite associated with the manual mixing and screen printing approach. Likewise, the simulated IL is 4.98 dB, whereas the measured insertion is 6.7 ± 2 dB. The measured 10-dB bandwidth of the device is 2.79 GHz, which can be further improved by implementing broadband microstrip feedline architectures such as in [22]. There are some discrepancies between the measured and simulated results, which are discussed further in the following.

A. Surface Roughness Measurement and Analysis

Bowrothu *et al.* [23] showed that when the roughness is greater than the skin depth of the conductor at the frequency of interest, it further adds additional loss to the device due to absorption and scattering of the fields at the irregular surface boundaries. Therefore, the average roughness of the screen-printed BaM/PDMS composite and PCB substrate is measured using a Brucker Optical Profilometer and plotted, as shown in Fig. 7. The measured average roughness of the BaM/PDMS composite surface and the PCB substrate is approximately 4 and 1 μm, respectively, which are far greater than the skin depth of copper at 35 GHz (∼350 nm). Due to this, the loss contribution associated with the surface roughness is not ignorable. Adding the surface roughness effects using the Groiss model [24], the structure is simulated again in HFSS and plotted in Fig. 8. After including roughness effects, total IL is 6.1 dB where an additional 1.1-dB loss is caused due to roughness effects. Other miscellaneous losses would be contact resistance loss, cable connector loss, and

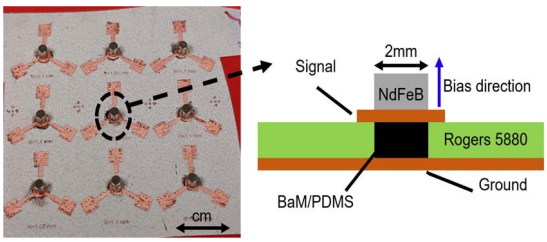

Fig. 9. Using NdFeB permanent bias magnets on fabricated devices.

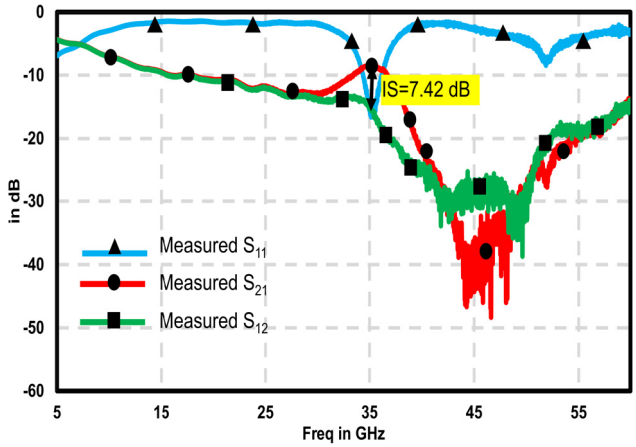

Fig. 10. Circulator performance using NdFeB permanent bias.

use of an inaccurate substrate loss parameter. Note that we used the substrate loss tangent value at 10 GHz provided by the vendor, while the device was operated at 35 GHz.

B. Effect of Magnetic Alignment on Circulator Performance

Although the BaM/PDMS composite was formed under a strong magnetic field during composite curing, the magnetic alignment of the BaM particles in the composite might not be ideal. Under ideal simulation conditions, it is assumed that the BaM/PDMS composite is fully saturated, and the applied dc static field is uniform across the sample in the Z-direction (OOP). However, in the case of self-biased circulators, the magnet operates near remanence instead of saturation, which causes more IL and a poor bandwidth [25]. Also, due to the nonellipsoidal shape of the ferrite, nonuniform demagnetization fields exist, especially strong around the edges of the circulator disk. The magnetic polarization of the device can be further improved with additional magnetic field application. Therefore, the external magnetic bias field is applied to the devices using a 2-mm-diameter NdFeB permanent magnets, as shown in Fig. 9. The resulting RF performance of these devices is measured and plotted in Fig. 10. Due to the external bias field applied by the permanent magnet, the IL of the device is decreased to 8.4 dB and the isolation is greatly improved, i.e., 7.42 dB at the resonance frequency. Isolation performance of the device biased with the additional magnet shows much closer performance to that of the simulated device.

C. Loss Analysis and Future Road Map of the Circulator

Losses in the circulator RF device are mainly categorized into four types, i.e., the conductor loss and radiation loss (C.L+R.L), the dielectric loss (D.L), the surface roughness loss (SR.L), and the magnetic linewidth loss (L.L). As it is challenging to differentiate them experimentally, using HFSS, the contribution of various losses on circulator performance is analyzed and summarized in Table II. It can be noted that nearly 2.3-dB IL and reduced isolation in the measurement results is due to the large magnetic linewidth of the fabricated ferrite composite. From [26], the IL and isolation depend on the squareness of the magnetic hysteresis, crystal size, grain orientation, porosity, and so on. Hence, the linewidth and isolation can be further improved by selecting better magnetic particles. Also, as PDMS suffers from high dielectric loss, the binding material can be switched to other polymers with lower RF loss tangent such as SU-8 and photopatternable epoxy that shows much less loss tangent compared with PDMS at mm-wave frequencies [27]. Likewise, surface roughness can be minimized by switching to substrates with smooth surface roughness, such as glass and fused silica. Recent work on the Cu/Co multilayer conductor has demonstrated better performance than a conventional copper counterpart in Ka-band [28]. Therefore, conductor loss can also be further reduced by transitioning from the conventional solid copper to the multilayer conductors.

TABLE II
LOSS ANALYSIS

Losses	Insertion loss (dB)	Isolation (dB)	Individual Loss (dB)
C.L+R.L	1.28	21.07	
C.L+R.L+D.L	2.57	17	D.L=1.29
C.L+R.L+D.L+L.L	4.88	8.62	L.L=2.31
C.L+R.L+D.L+L.L +SR.L	6.1	8.65	SR.L=1.2
Misc.	2.3		
Measured loss	8.42	7.42	

V. COMPARISON AND CONCLUSION

A 254-μm-thick BaM/PDMS composite consisting of thick magnetic BaM/PDMS composite is embedded in a Rogers 5880 substrate using screen printing for a circulator operated in the mm-wave frequency range. A circulator operating at 35 GHz is successfully designed, fabricated, and characterized. Performance of the circulator is measured with and without permanent bias magnets. Targeted and measured responses show good match in terms of return loss and isolation, especially with permanent biasing magnets. High IL is due to high loss tangent, large linewidth of BaM/PDMS, and surface roughness effects. Table III summarizes the comparison of various microfabricated self-biased circulators including one from this work, which is the only demonstrated low-temperature processed BaM/PDMS-based device, enabling it to be CMOS and organic board process compatible, and therefore giving it potential for integrable packaging compatible magnetics MMIC systems operating in mm-wave bands.

TABLE III
COMPARISON DATA

Ref.	Freq (GHz)	IL (dB)	IS (dB)	Proc. temp (°C)	Film thickness (μm)	10 dB BW (GHz)
[12]	47	6.9	1.5	850	10	1.86
[13]	40	17	2.6	800	10	-
[29]	26	27	44	1000	10	-
[30]	39.34	6.9	1.5	-	16	-
This work without bias	**35.2**	**8.7**	**3.9**	**70**	**254**	**2.79**
This work with bias	**35.4**	**8.42**	**7.42**	**70**	**254**	**3.11**

ACKNOWLEDGMENT

The authors would like to thank Rogers Corporation for the donation of the printed circuit board (PCB) substrate. They would also like to thank Dr. J. Lin for providing RF measurement equipment. Fabrication is performed at the Nanoscale Research Facility (NRF), University of Florida.

REFERENCES

[1] M. B. Yassein, S. Aljawarneh, and A. Al-Sadi, "Challenges and features of IoT communications in 5G networks," in *Proc. Int. Conf. Electr. Comput. Technol. Appl. (ICECTA)*, Nov. 2017, pp. 1–5.

[2] J. Govil and J. Govil, "4G mobile communication systems: Turns, trends and transition," in *Proc. Int. Conf. Converg. Inf. Technol. (ICCIT)*, Nov. 2007, pp. 13–18.

[3] G. A. Akpakwu, B. J. Silva, G. P. Hancke, and A. M. Abu-Mahfouz, "A survey on 5G networks for the Internet of Things: Communication technologies and challenges," *IEEE Access*, vol. 6, pp. 3619–3647, 2018.

[4] S. Tanaka, N. Shimomura, and K. Ohtake, "Active circulators—The realization of circulators using transistors," *Proc. IEEE*, vol. 53, no. 3, pp. 260–267, Mar. 1965.

[5] T. Dinc, A. Nagulu, and H. Krishnaswamy, "A millimeter-wave non-magnetic passive SOI CMOS circulator based on spatio-temporal conductivity modulation," *IEEE J. Solid-State Circuits*, vol. 52, no. 12, pp. 3276–3292, Dec. 2017.

[6] J.-F. Chang, J.-C. Kao, Y.-H. Lin, and H. Wang, "Design and analysis of 24-GHz active isolator and quasi-circulator," *IEEE Trans. Microw. Theory Techn.*, vol. 63, no. 8, pp. 2638–2649, Aug. 2015.

[7] T. Kodera, D. L. Sounas, and C. Caloz, "Magnetless nonreciprocal metamaterial (MNM) technology: Application to microwave components," *IEEE Trans. Microw. Theory Techn.*, vol. 61, no. 3, pp. 1030–1042, Mar. 2013.

[8] N. Aaron Estep, D. L. Sounas, and A. Alù, "Magnetless microwave circulators based on spatiotemporally modulated rings of coupled resonators," *IEEE Trans. Microw. Theory Techn.*, vol. 64, no. 2, pp. 502–518, Feb. 2016.

[9] E. Schloemann and R. E. Blight, "Broad-band stripline circulators based on YIG and Li-ferrite single crystals," *IEEE Trans. Microw. Theory Techn.*, vol. 34, no. 12, pp. 1394–1400, Dec. 1986.

[10] M. Pinto, L. Marzall, A. Ashley, D. Psychogiou, and Z. Popovic, "Design-oriented modelling of microstrip ferrite circulators," in *Proc. 48th Eur. Microw. Conf. (EuMC)*, Sep. 2018, pp. 215–218.

[11] G. Benito, M. P. Morales, J. Requena, V. Raposo, M. Vázquez, and J. S. Moya, "Barium hexaferrite monodispersed nanoparticles prepared by the ceramic method," *J. Magn. Magn. Mater.*, vol. 234, no. 1, pp. 65–72, Aug. 2001.

[12] F. K. H. Gellersen and A. F. Jacob, "A sol-gel approach for self-biased barium hexaferrite thin-film circulators," in *Proc. 46th Eur. Microw. Conf. (EuMC)*, Oct. 2016, pp. 361–364.

[13] A.-S. Dehlinger *et al.*, "Development of millimeter wave integrated circulator based on barium ferrite," *Mater. Sci. Eng., C*, vol. 28, nos. 5–6, pp. 755–758, Jul. 2008.

[14] Y. Chen, A. L. Geiler, T. Sakai, S. D. Yoon, C. Vittoria, and V. G. Harris, "Microwave and magnetic properties of self-biased barium hexaferrite screen printed thick films," *J. Appl. Phys.*, vol. 99, Apr. 2006, Art. no. 08M904.

[15] A. H. Sihvola and J. A. Kong, "Effective permittivity of dielectric mixtures," *IEEE Trans. Geosci. Remote Sens.*, vol. 26, no. 4, pp. 420–429, Jul. 1988.

[16] N. Zeina, H. How, and C. Vittoria, "Self-biasing circulators operating at Ka-band utilizing M-type hexagonal ferrites," *IEEE Trans. Magn.*, vol. 28, no. 5, p. 3219, Sep. 1992.

[17] J. Trajkovikj, J.-F. Zurcher, and A. K. Skrivervik, "Soft and flexible antennas on permittivity adjustable PDMS substrates," in *Proc. Loughborough Antennas Propag. Conf. (LAPC)*, Nov. 2012, pp. 1–4.

[18] N. J. Farcich, J. Salonen, and P. M. Asbeck, "Single-length method used to determine the dielectric constant of polydimethylsiloxane," *IEEE Trans. Microw. Theory Techn.*, vol. 56, no. 12, pp. 2963–2971, Dec. 2008.

[19] D. M. Pozar, *Microwave Engineering*, 3rd ed. Hoboken, NJ, USA: Wiley, 2005.

[20] G. Camino, S. M. Lomakin, and M. Lazzari, "Polydimethylsiloxane thermal degradation Part 1. Kinetic aspects," *J. Polym.*, vol. 42, no. 6, pp. 2395–2402, 2001.

[21] K. N. Ren, Y. Z. Zheng, W. Dai, D. Ryan, C. Y. Fung, and H. K. Wu, "Soft-lithography-based high temperature molding method to fabricate whole teflon microfluidic chips," in *Proc. 14th Int. Conf. Miniaturized Syst. Chem. Life Sci.*, Groningen, The Netherlands, Oct. 2010, Art. no. 554556.

[22] B. K. O'Neil and J. L. Young, "Design of self-biased, wideband microstrip circulators for integrated antenna systems," in *Proc. IEEE Antennas Propag. Soc. Int. Symp.*, Jul. 2008, pp. 1–4.

[23] R. Bowrothu, S. Hwangbo, T. Schumann, and Y.-K. Yoon, "28GHz through glass via (TGV) based band pass filter using through fused silica via (TFV) technology," in *Proc. IEEE 69th Electron. Compon. Technol. Conf. (ECTC)*, May 2019, pp. 695–699.

[24] S. Groiss, I. Bardi, O. Biro, K. Preis, and K. R. Richter, "Parameters of lossy cavity resonators calculated by the finite element method," *IEEE Trans. Magn.*, vol. 32, no. 3, pp. 894–897, May 1996.

[25] H. How *et al.*, "Influence of nonuniform magnetic field on a ferrite junction circulator," *IEEE Trans. Microw. Theory Techn.*, vol. 47, no. 10, pp. 1982–1989, Oct. 1999.

[26] V. G. Harris and A. S. Sokolov, "The self-biased circulator: Ferrite materials design and process considerations," *J. Supercond. Novel Magn.*, vol. 32, no. 1, pp. 97–108, Jan. 2019.

[27] N. Ghalichechian and K. Sertel, "Permittivity and loss characterization of SU-8 films for mmW and terahertz applications," *IEEE Antennas Wireless Propag. Lett.*, vol. 14, pp. 723–726, 2015.

[28] R. Bowrothu and Y. K. Yoon, "Low loss Cu/Co metaconductor based array antenna in Ka band for 5G applications," in *Proc. IEEE Antenna Propag. Symp.*, Jul. 2020, pp. 1–2.

[29] B. Peng, H. Xu, H. Li, W. Zhang, Y. Wang, and W. Zhang, "Self-biased microstrip junction circulator based on barium ferrite thin films for monolithic microwave integrated circuits," *IEEE Trans. Magn.*, vol. 47, no. 6, pp. 1674–1677, Jun. 2011.

[30] T. Boyajian, D. Vincent, S. Neveu, M. Le Berre, and J. Rousseau, "Coplanar circulator made from composite magnetic material," in *IEEE MTT-S Int. Microw. Symp. Dig.*, Jun. 2011, pp. 1–4.

Renuka Bowrothu (Member, IEEE) received the B.S. degree from the Vasavi College of Engineering, Hyderabad, India, in 2015, and the M.S. degree from the University of Florida, Gainesville, FL, USA, in 2017, where she is currently pursuing the Ph.D. degree in electrical and computer engineering.

Her current research interests include RF/microwave passive components designing, microscale/nanoscale fabrication, and low-loss RF conductors for 5G applications.

Mr. Bowrothu was a recipient of the IEEE Antennas and Propagation Society Doctoral Research Award in 2019.

Hae-In Kim (Member, IEEE) was born in South Korea in 1994. She received the B.S. degree from Gangneung-Wonju National University, Gangneung, South Korea, in 2017, and the M.S. degree from the University of Florida, Gainesville, FL, USA, in 2019, where she is currently pursuing the Ph.D. degree in electrical and computer engineering.

Her current research interests include microfabrication/nanofabrication, RF MEMS, RF/microwave passive components, and low RF loss conductors for 5G/millimeter-wave applications.

Connor S. Smith (Graduate Student Member, IEEE) received the dual B.S. degrees in electrical and computer engineering and the M.S. degree in electrical and computer engineering from The University of Alabama, Tuscaloosa, Al, USA, in 2016 and 2017, respectively. He is currently pursuing the Ph.D. degree in electrical and computer engineering at the University of Florida, Gainesville, FL, USA.

His research interests include magnetic nanocomposites, novel magnetic materials, magnetic microsystems, electromagnetics, and microfabrication.

David P. Arnold (Senior Member, IEEE) received the dual B.S. degrees in electrical and computer engineering and the M.S. degree in electrical and computer engineering from the University of Florida, Gainesville, FL, USA, in 1999 and 2001, respectively, and the Ph.D. degree in electrical and computer engineering from the Georgia Institute of Technology, Atlanta, GA, USA, in 2004.

He is currently the George Kirkland Engineering Leadership Professor and the Associate Chair for Research with the Department of Electrical and Computer Engineering, the Deputy Director of the NSF Multifunctional Integrated System Technology (MIST) Center, and a member of the UF Interdisciplinary Microsystems Group (IMG), University of Florida. He has coauthored over 200 refereed journal articles and conference publications and holds 22 U.S. patents. His research interests include microstructured/nanostructured magnetic materials, magnetic microsystems, electromechanical transducers, and miniaturized power/energy systems.

Dr. Arnold is a member of Tau Beta Pi and Eta Kappa Nu. His research innovations have been recognized by the 2008 Presidential Early Career Award in Science and Engineering (PECASE) and the 2009 DARPA Young Faculty Award. He is an active participant in the magnetics and MEMS communities, with ongoing involvement in various conference committees. He is serving on the Editorial Board of *Micromachines* and the *Journal of Micromechanics and Microengineering*.

Yong-Kyu Yoon (Member, IEEE) received the Ph.D. degree in electrical and computer engineering from the Georgia Institute of Technology, Atlanta, GA, USA, in 2004.

He held a post-doctoral researcher position at the Georgia Institute of Technology from 2004 to 2006. He was an Assistant Professor with the Department of Electrical Engineering, The State University of New York, Buffalo, NY, USA, from 2006 to 2010. He is currently a Professor and the Graduate Coordinator with the Department of Electrical and Computer Engineering, University of Florida, Gainesville, FL, USA. He had his sabbatical leave at Seoul National University, Seoul, South Korea, from July and December 2017. He has coauthored over 200 peer-reviewed publications. His current research interests include metamaterials for RF/microwave applications; micromachined millimeter-wave/terahertz antennas and waveguides; wireless telemetry systems for biomedical applications; microelectromechanical systems, nanofabrication, and energy storage devices; lab-on-a-chip devices; and ferroelectric materials for memory and tunable RF devices.

Dr. Yoon was a recipient of the NSF Early Career Development Award in 2008 and the SUNY Young Investigator Award in 2009.